Vol. 79 (1991) *ACTA PHYSICA POLONICA A* No 4

IR DISPERSION OF LIQUID CH_3I. I. OPTICAL CONSTANTS AND INTEGRATED INTENSITIES*

M.A. CZARNECKI AND J.P. HAWRANEK

Institute of Chemistry, University of Wrocław, F. Joliot-Curie 14, 50-383 Wrocław, Poland

(Received March 3, 1990)

The spectra of both components of the complex refractive index of liquid CH_3I were obtained in the infrared region using the thin film transmission method. Dispersion data and integrated intensities for principal bands were determined and discussed.

PACS numbers: 33.20.Ea, 33.70.Fd, 78.20.Dj, 78.30.Cp

1. Introduction

The IR spectrum of liquid CH_3I has been studied in a number of laboratories [1–3]. There is a wealth of published studies of vibrational and reorientational relaxation of CH_3I in the liquid phase by various spectroscopic techniques, reviewed by several authors [4–6]. There are, however, no complete literature data on optical constants, which is surprising, since the determination of accurate IR correlation functions and vibrational intensities requires their knowledge. At present, the optical constants measured using the ATR method by Crawford et al. [7] are available only for the ν_3 and ν_6 bands. In the same paper integrated intensities for these bands are also reported. Integrated intensities of principal bands of liquid CH_3I were also measured using the interferometric method by Orville–Thomas et al. [8, 9] as well as by Pratt and King [10]; unfortunately the results differ considerably. There are also available infrared intensities [11–13] for main bands of CH_3I in gas-phase as well as theoretical papers including dipole-moment derivatives [14, 15].

*This work was supported by the Polish Academy of Sciences.

In this work we report the complete spectrum of the complex refractive index of liquid CH_3I in the IR region, determined using the thin-film transmission technique described elsewhere [16, 17]. The imaginary part of the complex refractive index was used to calculate integrated intensities for all fundamental bands as well as for stronger overtones and combination bands.

2. Experimental

The IR transmission spectra were recorded on a Perkin–Elmer 180 IR spectrophotometer in a double-beam, open reference beam mode [16, 17]. The scan speed did not exceed $5\,cm^{-1}\,min^{-1}$. All precautions were taken to avoid mechanical, electronic or optical distortion to measured spectra. The resolution was maintained on the level of ca. $1\,cm^{-1}$ to keep the ratio of the spectral slit-width to half-width of the bands below 0.1, in order to minimize the slit-width distortion and to avoid the necessity of deconvolution [18]. The calibration of the wavenumber scale was checked by recording spectra of liquid indene and gas-phase spectra of NH_3. Several cells with thicknesses ranging from 6.06 to 22.82 μm were used. The windows made of KBr, NaCl and CsI were ground and polished to high flatness, monitored in sodium light on a optical flat glass. The spacers were prepared out of teflon and aluminium foils of appropriate thicknesses. For thinest cells ($d < 10\mu m$) the geometrical parameters of the cell cavity were determined by fitting the experimental interference fringe pattern of the empty cell with the theoretical one, using the computational procedure described elsewhere [16, 17].

The spectra of CH_3I were recorded at controlled temperature of $298 \pm 1\,K$. Each spectrum was recorded several times in a particular cell, then the runs were digitized with a step of $1\,cm^{-1}$ and averaged. Analytical grade CH_3I was further purified by fractional distillation and dried over freshly prepared molecular sieves. The density of the liquid CH_3I was $d_{298} = 2.2650\ g/cm^3$, which corresponds to a molar concentration $c = 15.96\ mol/dm^3$.

3. Processing of spectra

From the thin-film transmission spectra recorded as described above, the spectra of real and imaginary components of the complex refractive index

$$\hat{n}(\nu) = n(\nu) + ik(\nu) \tag{1}$$

were determined. The computational procedure was based on the iterative dispersion-distortion correction procedure [16, 17]. It involves the subtractive Kramers – Kronig transformation in each step of the iteration. The transmission spectra were processed in segments of a width ranging from $900\,cm^{-1}$ to $150\,cm^{-1}$ following the cascade strategy. The anchor point for the first segment was taken from literature data [7] at $1010.0\,cm^{-1}$. For each subsequent segment of the spectrum the reference point was selected from the preceding section, already processed. In order to minimize truncation errors connected with the Kramers–Kronig transformation,

the beginning and the end of each segment were selected in non-absorbing regions [16, 17].

From the spectrum of the complex refractive index, the spectrum of the complex dielectric function

$$\hat{\varepsilon}(\nu) = \varepsilon'(\nu) + i\varepsilon''(\nu) \tag{2}$$

was obtained from Maxwell's relations throughout the entire IR region.

4. Results and discussion

4.1 Optical constants

Methyl iodide has nine vibrational modes: three totally symmetric (A_1) modes: ν_1 (sym.–CH_3 stretch.), ν_2 (sym.–CH_3def.), ν_3 (C–I stretch.) and three doubly degenerate E-type modes: ν_4 (asym.–CH_3 stretch.), ν_5 (asym.–CH_3 def.), ν_6 (–CH_3 rock.). All modes are both IR and Raman active. Apart from these fundamentals, some overtones and combination bands appear in the mid-IR region.

Thin-film transmission spectra of liquid CH_3I were obtained in the 4000–450 cm^{-1} range. In Figs. 1, 3, 5, 7 and 9 the transmission spectra in selected regions with prominent bands are shown. The corresponding spectra of both components of the refractive index are shown in Figs. 2, 4, 6, 8 and 10, respectively.

Basic dispersion data of principal IR absorption bands of liquid CH_3I are collected in Table I. Regions including only very weak bands were not included in the figures and in Table I, although data for the entire IR range were obtained. In Table I ν_r and n_r denote the position and the value of the refractive index at selected anchor points required for the Kramers–Kronig procedure; ν_e are wavenumbers of extremal points at the absorption curves ($k_{max}, \varepsilon''_{max}$) and corresponding dispersion curves (n_{min}, n_{max} and $\varepsilon'_{min}, \varepsilon'_{max}$). In brackets the errors (mean deviations) are given (in 10^{-4}). The values of k_{max} obtained for the ν_3 and ν_6 bands are in good agreement with literature data [7]. The description of fundamental vibrations of CH_3I was taken from literature [1–3].

As can be seen from Table I, most bands of liquid CH_3I are weak and dispersion extrema occur at the same position for the $\hat{n}(\nu)$ and $\hat{\varepsilon}(\nu)$ curves within experimental error, except for the moderate strength band ν_2. The dispersion amplitudes ($n_{max} - n_{min}, \varepsilon'_{max} - \varepsilon'_{min}$) of isolated bands are generally smaller than the corresponding absorption maxima ($k_{max}, \varepsilon''_{max}$), which is typical of absorption-dispersion curves deviating from the classical damped-harmonic oscillator behaviour.

4.2 Integrated intensities

The spectrum of $k(\nu)$ was used to calculate two kinds of integrated intensities for all fundamental bands as well as for stronger overtones and combination bands:

$$A = (4\pi/c) \int_{\nu_1}^{\nu_h} \nu k(\nu) d\nu \tag{3}$$

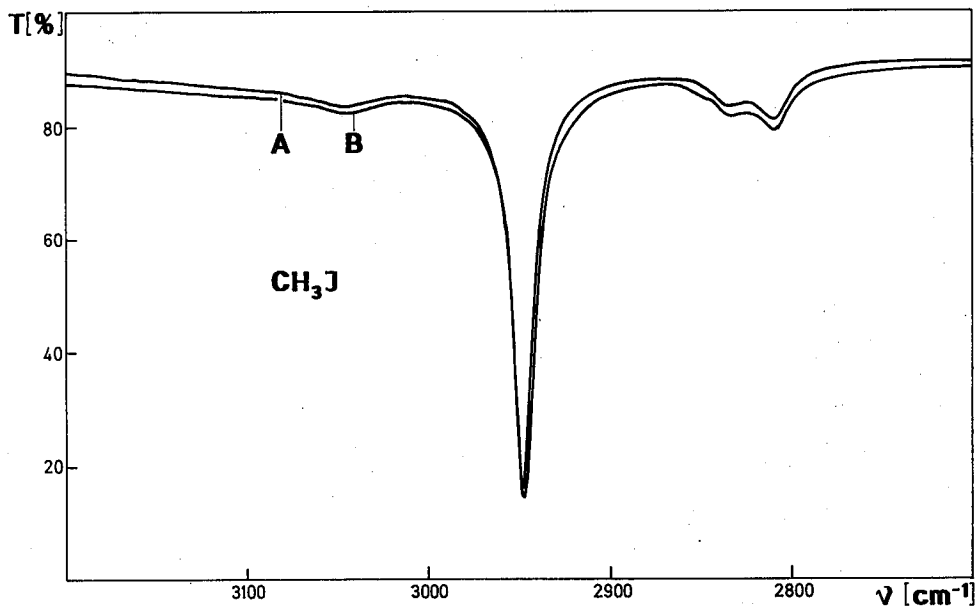

Fig. 1. Transmission spectra of liquid CH_3I in the 3200–2700 cm^{-1} range.
A — 21.56 μm (NaCl); B — 22.82 μm (KBr).

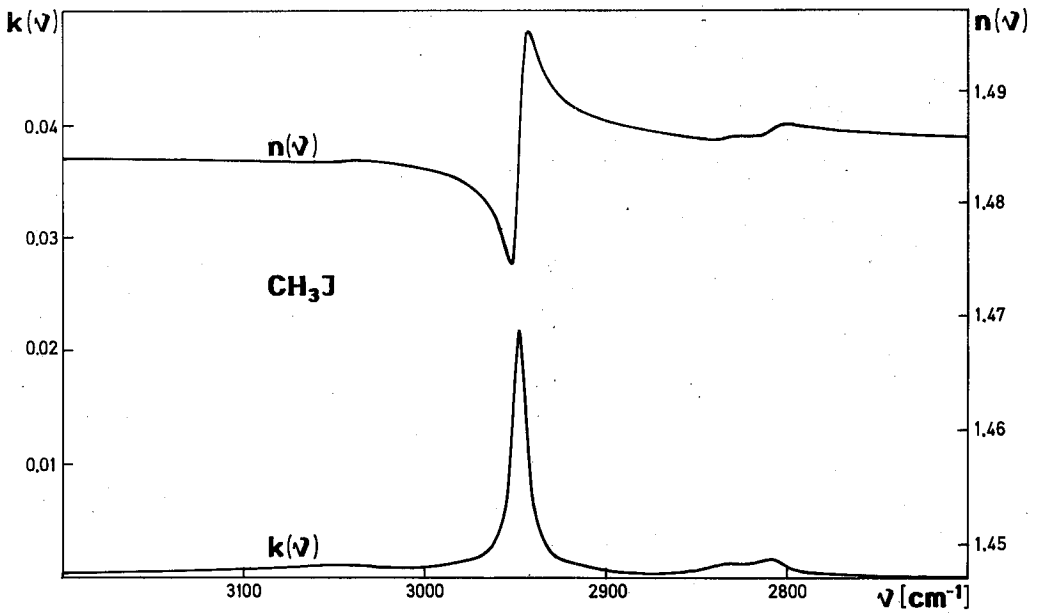

Fig. 2. The $\hat{n}(\nu)$ spectrum of liquid CH_3I in the 3200–2700 cm^{-1} range.

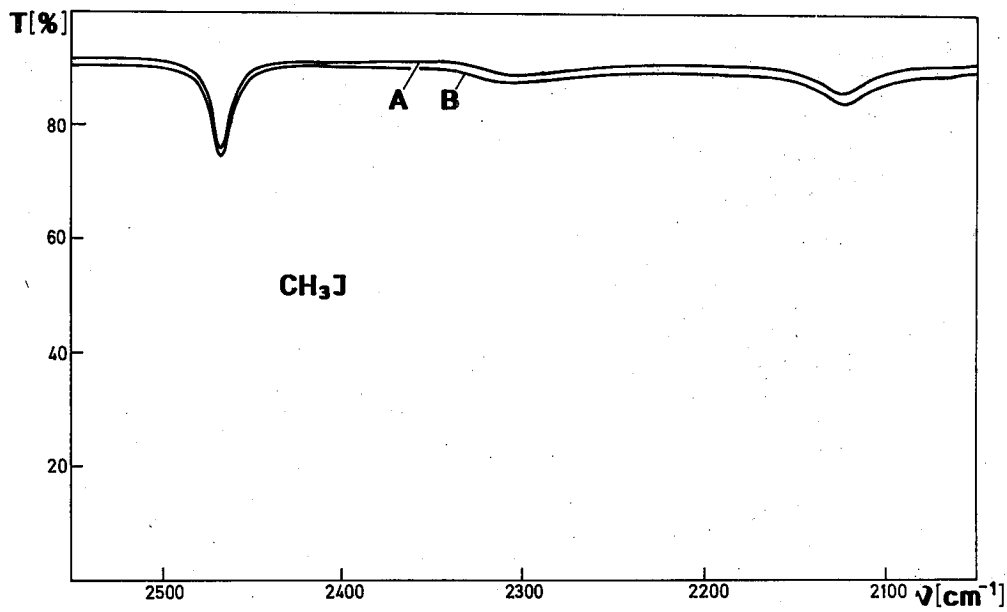

Fig. 3. Transmission spectra of liquid CH_3I in the 2550–2050 cm^{-1} range.
A — 21.56 μm (NaCl); B — 22.82 μm (KBr).

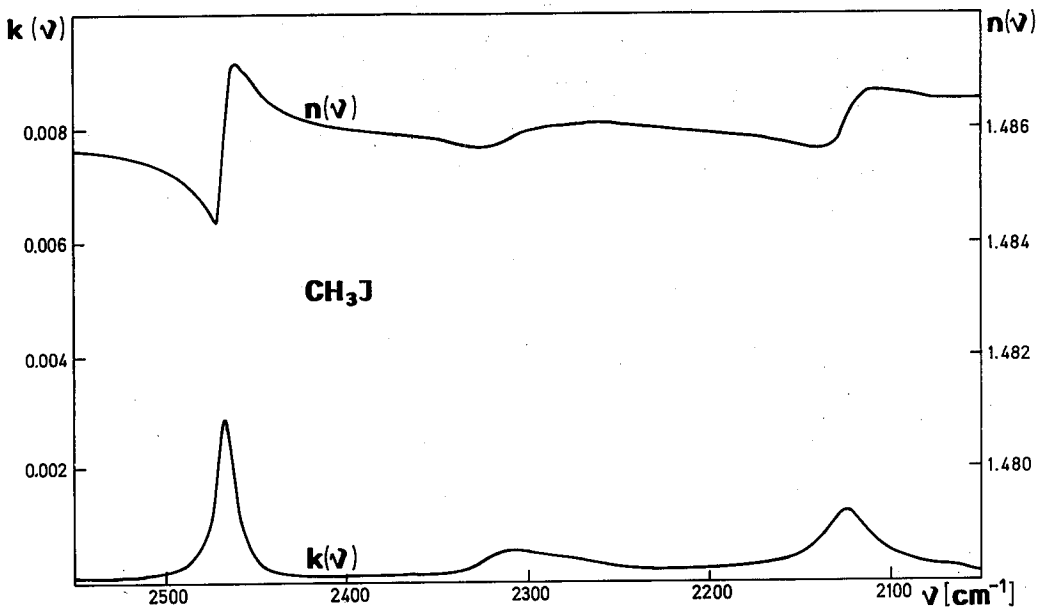

Fig. 4. The $\hat{n}(\nu)$ spectrum of liquid CH_3I in the 2550–2050 cm^{-1} range.

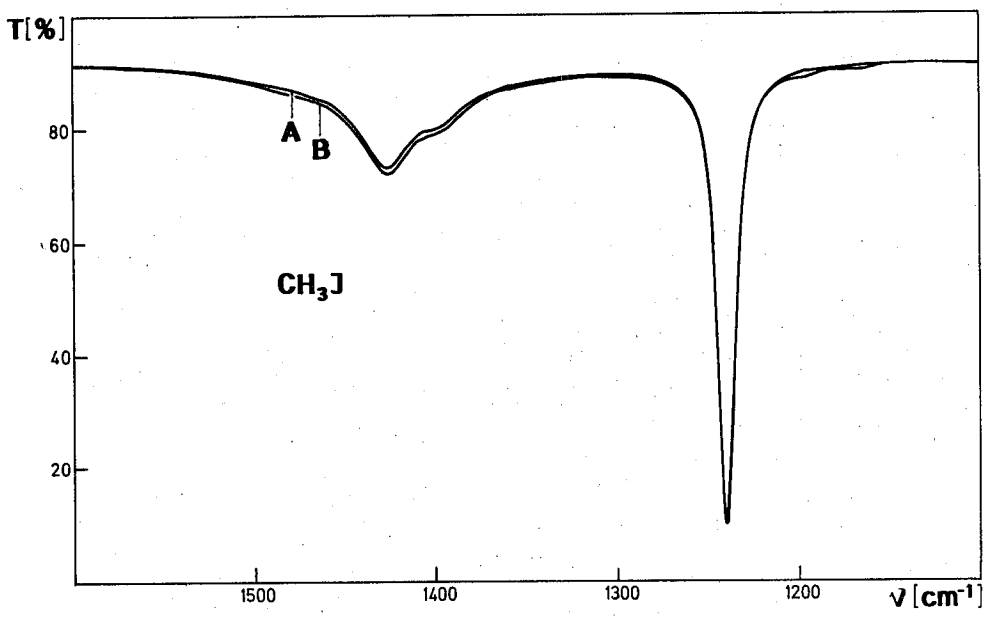

Fig. 5. Transmission spectra of liquid CH_3I in the 1600–1100 cm^{-1} range.
A — 6.06 μm (NaCl); B — 6.39 μm (KBr).

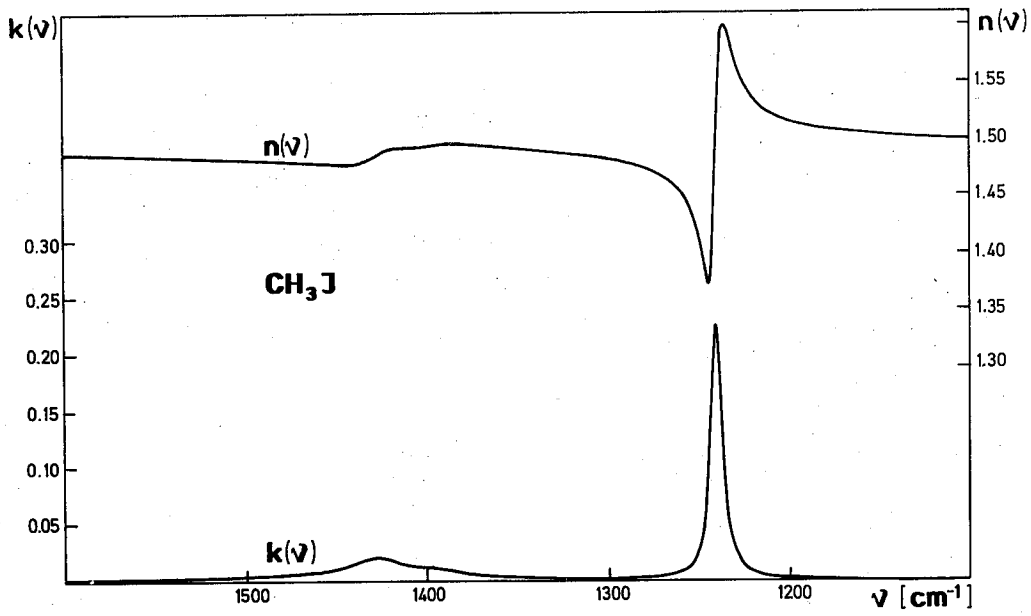

Fig. 6. The $\hat{n}(\nu)$ spectrum of liquid CH_3I in the 1600–1100 cm^{-1} range.

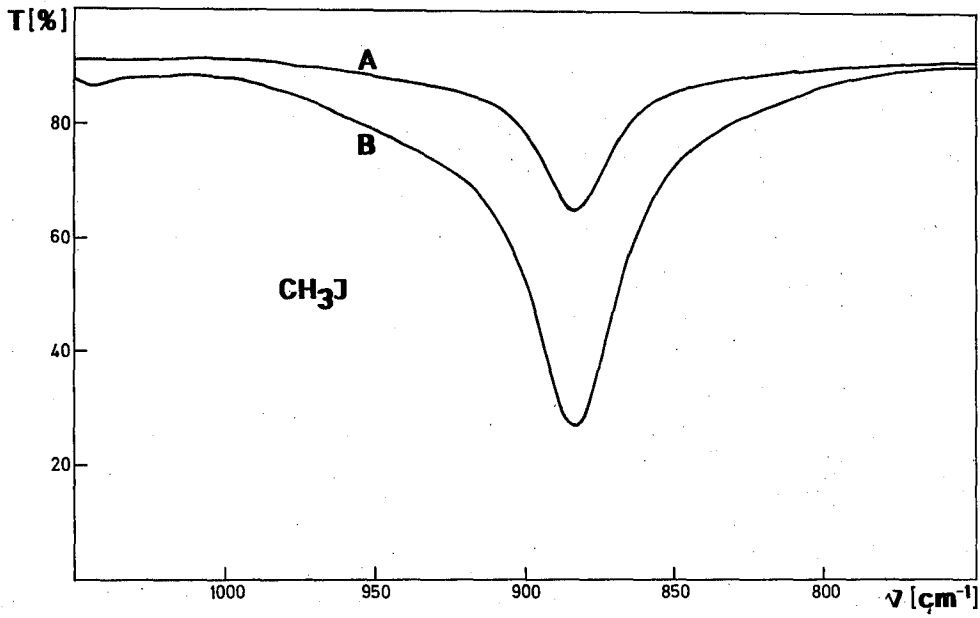

Fig. 7. Transmission spectra of liquid CH_3I in the 1050–750 cm^{-1} range.
A — 6.39 μm (KBr); B — 22.82 μm (KBr).

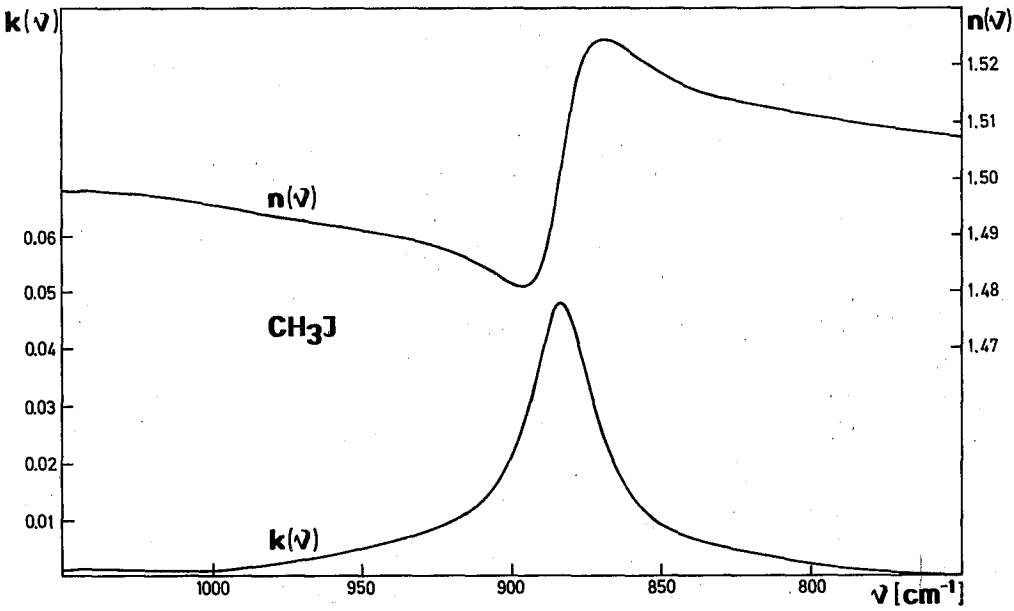

Fig. 8. The $\hat{n}(\nu)$ spectrum of liquid CH_3I in the 1050–750 cm^{-1} range.

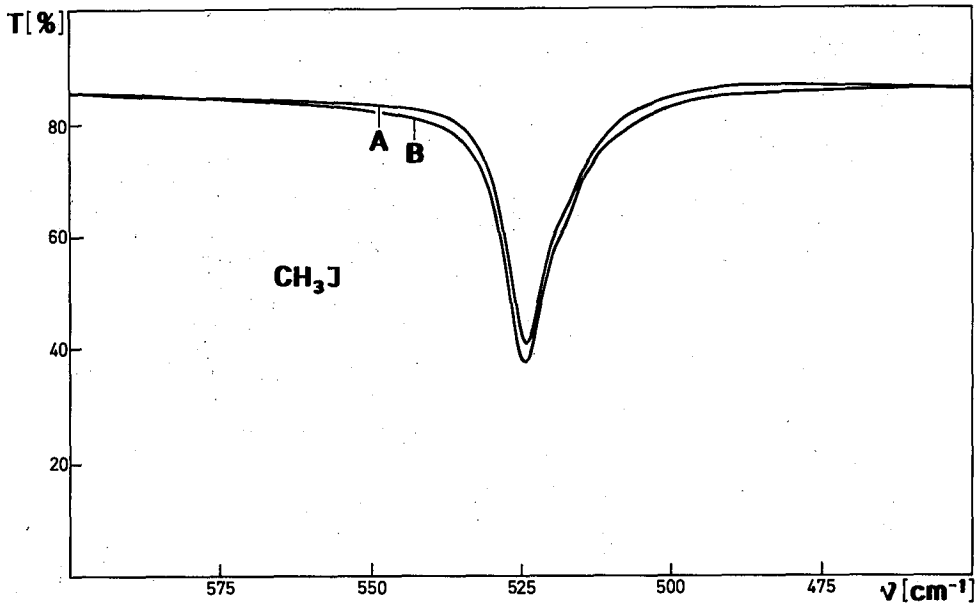

Fig. 9. Transmission spectra of liquid CH_3I in the 600–450 cm^{-1} range.
A — 19.94 μm (CsI); B — 21.82 μm (CsI).

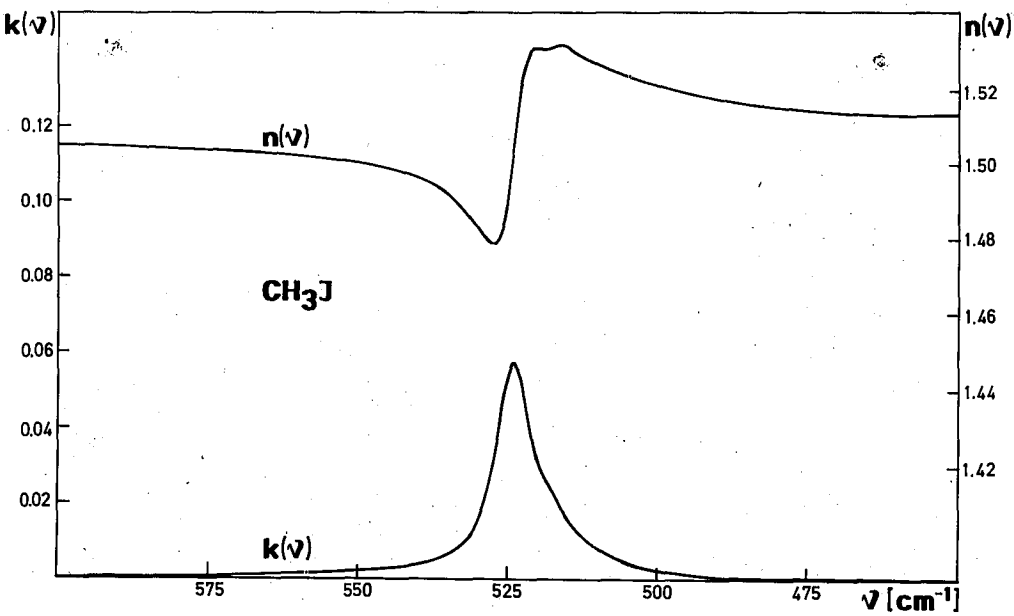

Fig. 10. The $\hat{n}(\nu)$ spectrum of liquid CH_3I in the 600–450 cm^{-1} range.

TABLE I

Dispersion data for principal IR bands of liquid CH_3I, $T = 298$ K.

Exp. range [cm^{-1}] Cell thickness [μm] ν_r [cm^{-1}], n_r	Mode	Dispersion data		
		ν_e [cm^{-1}]	n(min) k(max) n(max)	ε'(min) ε''(max) ε'(max)
1	2	3	4	5
4000–3850		3931.5	1.4873(1)	2.2121(1)
21.56 (NaCl)	$\nu_4 + \nu_6$	3922.0	0.0013(1)	0.0038(1)
22.82 (KBr)	(A_1+A_2+E)	3909.0	1.4885(1)	2.2157(1)
3495.0, 1.48792				
3520–2600		3053.0	1.4873(1)	2.2119(2)
21.56 (NaCl)	ν_4(E)	3043.0	0.0012(1)	0.0036(1)
22.82 (KBr)		3038.5	1.4874(1)	2.2124(2)
2580.0, 1.48922		2954.0	1.4780(1)	2.1842(5)
	$\nu_1(A_1)$	2950.5	0.0218(1)	0.0649(2)
		2945.5	1.4989(1)	2.2466(3)
		2843.0	1.4892(1)	2.2178(2)
	$2\nu_5$(A_1+E)	2833.5	0.0013(1)	0.0040(2)
		2828.0	1.4896(1)	2.2189(2)
		2820.5	1.4896(1)	2.2188(2)
	$\nu_5 + \nu_6 + \nu_3$	2810.0	0.0017(1)	0.0052(2)
	(A_1+A_2+E)	2803.0.	1.4906(1)	2.2220(2)
2600–1900		2472.0	1.4879(2)	2.2140(5)
21.56 (NaCl)	$2\nu_2(A_1)$	2467.0	0.0029(1)	0.0086(1)
22.82 (KBr)		2461.0	1.4907(1)	2.2223(2)
1610.0, 1.48953		2140.0	1.4892(1)	2.2177(3)
	$\nu_2 + \nu_6$(E)	2123.0	0.0013(1)	0.0037(3)
		2105.5	1.4902(1)	2.2208(3)
1630–1070		1445.0	1.4786(21)	2.1862(63)
6.06 (NaCl)	ν_5(E)	1426.5	0.0212(1)	0.0632(5)
1065.0, 1.49906		1409.5	1.4937(19)	2.2309(58)
1620–750		1243.0	1.3729(20)	1.8701(51)
6.39(KBr)	$\nu_2(A_1)$	1240.0	0.2265(3)	
1010.0, 1.4960		1239.0		0.6832(18)
		1235.0	1.6015(8)	2.5551(23)
1620–750		896.5	1.4801(15)	2.1901(43)
6.39 (KBr)	ν_6(E)	883.0	0.0479(1)	0.1441(5)
1070–720		870.0	1.5244(13)	2.3231(39)
22.82 (KBr)				
1010.0, 1.4960				
600–450		527.0	1.4776(1)	2.1821(4)
19.94 (CsI)	$\nu_3(A_1)$	524.0	0.0577(4)	0.1737(4)
21.82 (CsI)		516.0	1.5304(2)	2.3418(5)
770.0, 1.50701				

TABLE II

Integrated intensities (A_i), for selected bands of liquid CH_3I, in units of 10^6 cm mol^{-1}.

Mode (ν_0)	A_i (this work) $\nu_h - \nu_l$(cm^{-1})	Literature data		
		A_i	Method	Ref.
1	2	3	4	5
$\nu_4 + \nu_6$ (3922.5)	0.096(4)	–		
	3985–3860			
ν_4 (3043.0)	0.243(1)*	0.26	I	[8]
	0.314(5)			
	3335–3010			
ν_1 (2950.5)	0.759(4)*	1.31	I	[8]
	0.879(4)	0.99	I	[9]
	3010–2870	0.86	I	[10]
$2\nu_5$ (2833.5)	0.150(8)*	0.19	I	[8]
$\nu_5 + \nu_6 + \nu_3$ (2810.0)	0.175(6)	0.16	I	[9]
	2870–2720			
$2\nu_2$ (2467.0)	0.094(1)	0.25	I	[8]
	2530–2405	0.13	I	[9]
$\nu_5 + \nu_6$ (2303.0)	0.142(1)	–		
$\nu_2 + \nu_6$ (2123.0)	2380–2045			
ν_5 (1426.5)	1.481(26)	2.81	I	[8]
	1600–1300	2.26	I	[9]
		2.19	I	[10]
ν_2 (1240.0)	2.450(20)	3.05	I	[8]
	1300–1140	3.18	I	[9]
		2.90	I	[10]
ν_6 (883.0)	1.500(1)	2.12	I	[8]
	1010–745	2.04	I	[9]
		1.43	I	[10]
		1.74	ATR	[7]
ν_3 (524.0)	0.304(3)	1.18	I	[8]
	595–455	0.38	I	[9]
		0.38	ATR	[7]

* intensities obtained from the numerical separation.

TABLE III

Comparison of band intensities (Γ) in liquid- and gas-phase for CH_3I.

Mode (ν_0^l)	$\Delta\nu_{1/2}$ [cm^{-1}]	$\Gamma[10^3 cm^2 mol^{-1}]$ This work	Gas-phase (ν_0^g)	Γ_l/Γ_g	Ref.
ν_1 (2950.5)	10.4	0.298(1)	0.371 (2970)	0.80	[12]
			0.403	0.74	[13]
ν_2 (1240.0)	7.6	1.977(16)	1.651 (1251)	1.20	[12]
			1.913	1.03	[13]
ν_3 (524.0)	7.1	0.580(4)	0.362 (533)	1.60	[12]
			0.365	1.59	[13]
ν_4 (3043.0)	≈ 66	0.101(1)	0.070 (3061)	1.44	[12]
			0.066	1.53	[13]
ν_5 (1426.5)	54.3	1.038(18)	0.736 (1440)	1.41	[12]
			0.572	1.81	[13]
ν_6 (883.0)	28.4	1.694(1)	1.012 (880)	1.67	[12]
			0.909	1.86	[13]
$2\nu_5$ (2833.5)*	≈ 30	0.062(2)	0.054 (2861)	1.15	[12]
			0.070	0.89	[13]

* half-width for $2\nu_5$ band, intensity including the $\nu_5+\nu_6+\nu_3$ band at 2810.0 cm^{-1} (as in gas-phase).

and

$$\Gamma = (4\pi/c)\int_{\nu_l}^{\nu_h} k(\nu)\mathrm{d}\nu, \tag{4}$$

where c is the concentration (in mol/dm^3) in the pure liquid, ν denotes a wavenumber, ν_h and ν_l – high and low wavenumber limits of integration, respectively. The numerical integration was carried out using both the trapezium formula and Simpson's formula, with the same integration interval of 1 cm^{-1}; the discrepancies were much less than the experimental errors given in brackets. Wavenumber limits of the integration were selected in non-absorbing regions of the spectrum. During calculation of the integral the background of the $k(\nu)$ curve was approximated by a straight line between ν_h and ν_l and subtracted.

The absorption bands are considerably overlapping in some spectral regions. In order to obtain infrared intensities and other spectral parameters of individual bands, it was necessary to make a careful numerical separation into individual bands. For this purpose we used modified Levenberg's least squares iteration method [19, 20]. The band shapes were approximated by a Cauchy–Gauss product function:

$$A(\nu) = a_1\left[1 + a_2^2(\nu - a_3)^2\right]^{-1}\exp\left[-a_4^2(\nu - a_3)^2\right], \tag{5}$$

where a_1 is the peak height, a_3 — the peak wavenumber and a_2, a_4 — the band-shape parameters. The calculated parameters of individual bands were used to determine integrated intensities and other spectral parameters. For the bands, for

which spectral parameters have been obtained from numerical separation, the integrals were calculated in the limits of $\nu_0 \pm 15b$, where b is the semi-half width of the band (i.e. $\Delta\nu_{1/2} = 2b$).

The band envelope depicted in Fig. 2, consisting of the ν_4, ν_1, $2\nu_5$ and $\nu_5 + \nu_6 + \nu_3$ bands, is especially cumbersome. The high-frequency wing of the ν_4 band extends up to 3335 cm^{-1}. Two sets of integrals are given in Table II for this block: one calculated by direct integration in the specified limits, the second one obtained by numerical band separation and subsequent integration as described above. In both cases the baseline was assumed to be linear between the limiting points of the envelope, i.e. 3335–2720 cm^{-1}.

If a fundamental band is considerably overlapping with an overtone or a combination band of corresponding symmetry, they are in resonance and the weaker band usually "borrows" intensity from the fundamental band. In this case we assume that the entire intensity belongs to the fundamental band (see ν_3 and ν_5). It seems to be more reasonable than numerical separation which in such cases gives unreliable values.

In Table II integrated intensities (A) are collected and compared with literature data [7–10]; mean deviations (in 10^{-3}) are given in brackets. As can be seen from Table II, our results are in reasonable agreement with the results obtained by ATR method [7] for the ν_3 and ν_6 bands. The agreement is much worse with results determined by the interferometric method [8–10], which seem to be overvalued. Furthermore, the results obtained by the interferometric method by Pratt and King [10] and Pritchard and Orville–Thomas [8] differ considerably; for most of the fundamental bands there is about 40% disagreement. Using a modified procedure Ramsey, Ladd and Orville–Thomas [9] recalculated the data obtained earlier [8]. The agreement was a little better but still unsatisfactory.

In Table III we compared peak positions and integrated intensities (Γ) with literature data for the gas-phase [11–13]. Most of bands show greater integrated intensities in liquid-phase than in gas-phase, except the ν_1 band. It may arise to some extent as a result of difficulties in the evaluation of the integral for ν_1 as discussed above. As can be seen, most of the bands of liquid CH_3I lie at lower wavenumbers than in the gas-phase (about 10–20 cm^{-1}), whereas the ν_3 band lies in the liquid-phase at higher wavenumber than in the gas-phase (about 3 cm^{-1}).

Using the Polo–Wilson formula [21]:

$$\frac{\Gamma_l}{\Gamma_g} = \frac{1}{n}\left(\frac{n^2+2}{3}\right)^2, \tag{6}$$

one can calculate the theoretical ratio of band intensities in the liquid-phase (Γ_l) to those in the gas-phase (Γ_g). Taking as the average refractive index $n \approx 1.49$, the ratio ought to be about 1.33. For the vibrations ν_2 and $2\nu_5$ the ratio is smaller than the theoretical one, while for vibrations ν_3, ν_4, ν_5 and ν_6 it is larger. For the ν_1 vibration the ratio considerably differs from this one calculated from formula (5).

A deeper understanding of the integrated intensities and their dependence on the type of vibration requires reliable results of theoretical calculations. Unfortu-

nately, the comparison between the theoretical results [14, 15] and the gas-phase data [12] is not encouraging. Even more difficult is the discussion of intensity changes between the gas- and liquid-phase.

As can be seen from Table III, the E-type bands are considerably broader than the A_1 bands. This is due not only to the degeneracy of the E-bands, but also to the increased contribution of reorientational relaxation in the broadening of these perpendicular bands, resulting from a faster spinning motion of the molecule around the C_3 axis as compared with the tumbling motion around both remaining axes [4–6, 22–24]. This was observed also for previously studied CCl_3CN [25].

Acknowledgments

We wish to thank Mr. P. Faleński for assistance.

References

[1] W.K. Glass, A.D.E. Pullin, *Trans. Faraday Soc.* **59**, 25 (1963).

[2] P.F. Fenlon, F.F. Cleveland, A.G. Maister, *J. Chem. Phys.* **19**, 1561 (1951).

[3] I.L. Mador, R.S. Quinn, *J. Chem. Phys.* **20**, 1837 (1952).

[4] G.J. Evans, M.W. Evans, *J. Mol. Liq.* **25**, 177 (1983).

[5] W.G. Rothschild, *Dynamics of Molecular Liquids*, John Wiley, New York (1984).

[6] M.W. Evans, G.J. Evans, *Adv. Chem. Phys.* **63**, 377 (1985).

[7] C.E. Favelukes, A.A. Clifford, B. Crawford, *J. Phys. Chem.* **72**, 962 (1968).

[8] W.H. Pritchard, W.J. Orville–Thomas, *Trans. Faraday Soc.* **61**, 1549 (1965).

[9] J.A. Ramsey, T.A. Ladd, W.J. Orville–Thomas, *J. Chem. Soc. Faraday Trans. II* **68**, 193 (1972).

[10] H.A. Pratt, W.T. King, *J. Chem. Phys.* **47**, 3361 (1967).

[11] J.W. Russel, C.D. Nedham, J. Overend, *J. Chem. Phys.* **45**, 3383 (1966).

[12] D.A. Dickson, I.M. Mills, B. Crawford Jr., *J. Chem. Phys.* **27**, 445 (1957).

[13] G.M. Barrow, D.C. Mc Kean, *Proc. R. Soc. Lond. A, Math. Phys. Sci.* **213**, 27 (1952).

[14] G. Berthier, *Isr. J. Chem.* **19**, 276 (1980).

[15] L.M. Sverdlov, *Opt. Spectrosc.* **6**, 729 (1959).

[16] J.P. Hawranek, P. Neelakantan, R.P. Young, R.N. Jones, *Spectrochim. Acta A, Mol. Spectrosc.* **32**, 75, 85 (1976).

[17] J.P. Hawranek, R.N. Jones, *Spectrochim. Acta A, Mol. Spectrosc.* **32**, 99, 111 (1976).

[18] K.S. Seshadri, R.N. Jones, *Spectrochim. Acta* **19**, 1013 (1963).
[19] K. Levenberg, *Q. Appl. Math.* **2**, 164 (1944).
[20] J.P. Hawranek, L. Sobczyk, *Acta Phys. Pol.* **A39**, 639 (1971).
[21] R.S. Polo, M.K. Wilson, *J. Chem. Phys.* **23**, 2376 (1955).
[22] G. Dreyfus, C. Breuillard, T. Nguyen Tan, A. Grosjean, J. Vincent–Geisse, *J. Mol. Struct.* **47**, 41 (1978).
[23] K. Tanabe, J. Hiraishi, *Spectrochim. Acta A, Mol. Spectrosc.* **36**, 665 (1980).
[24] R.M. Lynden–Bell, *Mol. Phys.* **33**, 907 (1977).
[25] M.A. Czarnecki, J.P. Hawranek, *J. Mol. Liquids* **46**, 151 (1990).